Biomaterials Science

PAPER

View Article Online
View Journal | View Issue

Cite this: *Biomater. Sci.*, 2017, **5**, 2093

In vitro and *in vivo* analysis of visible light crosslinkable gelatin methacryloyl (GelMA) hydrogels†

Iman Noshadi,‡[a,b,c] Seonki Hong,‡[a,b,c,d] Kelly E. Sullivan,[e] Ehsan Shirzaei Sani,[f] Roberto Portillo-Lara,[f,g] Ali Tamayol,[a,b,c] Su Ryon Shin,[a,b,c] Albert E. Gao,[e] Whitney L. Stoppel,[e] Lauren D. Black III,[e,h] Ali Khademhosseini *[a,b,c,i] and Nasim Annabi *[a,b,c,f]

Photocrosslinkable materials have been frequently used for constructing soft and biomimetic hydrogels for tissue engineering. Although ultraviolet (UV) light is commonly used for photocrosslinking such materials, its use has been associated with several biosafety concerns such as DNA damage, accelerated aging of tissues, and cancer. Here we report an injectable visible light crosslinked gelatin-based hydrogel for myocardium regeneration. Mechanical characterization revealed that the compressive moduli of the engineered hydrogels could be tuned in the range of 5–56 kPa by changing the concentrations of the initiator, co-initiator and co-monomer in the precursor formulation. In addition, the average pore sizes (26–103 μm) and swelling ratios (7–13%) were also shown to be tunable by varying the hydrogel formulation. *In vitro* studies showed that visible light crosslinked GelMA hydrogels supported the growth and function of primary cardiomyocytes (CMs). In addition, the engineered materials were shown to be biocompatible *in vivo*, and could be successfully delivered to the heart after myocardial infarction in an animal model to promote tissue healing. The developed visible light crosslinked hydrogel could be used for the repair of various soft tissues such as the myocardium and for the treatment of cardiovascular diseases with enhanced therapeutic functionality.

Received 8th February 2017,
Accepted 4th July 2017

DOI: 10.1039/c7bm00110j

rsc.li/biomaterials-science

Introduction

Hydrogels have been widely used in tissue engineering and regenerative medicine as artificial scaffolds, mimicking the extracellular matrix (ECM) surrounding the cells.[1] Their high water content, tunable chemical and physical properties, and ability to encapsulate cells, bio-macromolecules (*e.g.*, peptides/proteins, nucleotides, and antibodies), and therapeutic agents open up a variety of potential applications.[1–4] In particular, biopolymers that allow *in situ* sol–gel transition could be used to develop injectable materials, which can be delivered locally in a minimally invasive and cost-effective manner.[5] Injectable hydrogels made of natural or synthetic polymers have been widely reported, and shown to exhibit both advantages and drawbacks.[5,6] For instance, natural hydrogels such as hyaluronic acid, chitosan, alginate, and chondroitin sulfate have been extensively used due to their biocompatibility and biodegradability, but are limited by their low mechanical properties, as well as difficulties in tuning their degradation rate and biological functions.[4,6] On the other hand, synthetic polymer-based hydrogels such as poly(ethylene glycol) (PEG) and poly(vinyl alcohol) (PVA) have high mechanical strength

[a]*Biomaterials Innovation Research Center, Department of Medicine, Brigham and Women's Hospital, Harvard Medical School, Cambridge, MA 02139, USA. E-mail: n.annabi@neu.edu, alik@bwh.harvard.edu*
[b]*Harvard-MIT Division of Health Sciences and Technology, Massachusetts Institute of Technology, Cambridge, MA 02139, USA*
[c]*Wyss Institute for Biologically Inspired Engineering, Harvard University, Boston, MA 02115, USA*
[d]*Department of Emerging Materials Science, Daegu Gyeongbuk Institute of Science and Technology (DGIST), Daegu, 42988, Republic of Korea*
[e]*Department of Biomedical Engineering, Tufts University, Medford, MA 02155, USA*
[f]*Department of Chemical Engineering, Northeastern University, Boston, MA, 02115-5000, USA*
[g]*Tecnologico de Monterrey, Escuela de Ingeniería y Ciencias, Ave. Eugenio Garza Sada 2501, Monterrey, N.L., México, 64849*
[h]*Cellular, Molecular, and Developmental Biology Program, Sackler School for Graduate Biomedical Sciences, Tufts University School of Medicine, Boston, MA 02111, USA*
[i]*Nanotechnology Center, King Abdulaziz University, Jeddah 21569, Saudi Arabia*
†Electronic supplementary information (ESI) available. See DOI: 10.1039/c7bm00110j
‡These authors contributed equally to this work.

with a tunable microstructure, but often suffer from a lack of biological moieties.[4,6] Thus, there is a need for the development of hydrogels that combine the advantages of both natural and synthetic polymers.[7]

Light-induced photocrosslinking has been widely used for the fabrication of cell-laden injectable hydrogels with rapid gelation time and tunable physical properties.[8] Ultraviolet (UV) light is commonly used for the photocrosslinking of such materials, as well as in commercial products for dental applications. We have recently reported the engineering of highly elastic hydrogels *via* the UV light-mediated crosslinking of chemically modified tropoelastin or elastin-like polypeptides for wound healing and cardiac tissue engineering.[9–12] These UV crosslinked hydrogels exhibited high cytocompatibility for three-dimensional (3D) encapsulated cells *in vitro*, as well as negligible immune responses after subcutaneous implantation in rats.[13] In addition, UV crosslinked gelatin methacryloyl (GelMA)-based hydrogels have been used as 3D cell-laden hydrogels to promote *in vitro* vascularization and tissue formation.[14–16] Although we have shown that subcutaneous injection of cell laden GelMA hydrogels into rats led to vascular network formation and tissue healing,[17] *in situ* UV crosslinking of GelMA prepolymers may negatively impact the normal functioning of sensitive tissues such as the myocardium. The clinical translation of UV crosslinkable hydrogels as injectable materials for soft tissue regeneration has been limited owing to the biosafety concerns associated with the use of UV light. UV light may generate reactive oxygen species (ROS), which may induce endogenous oxidative damage to DNA (*e.g.*, dimerization or hydroxylation of bases) and cause accelerated tissue aging or cancer.[18] Other studies have reported that oxidative DNA alterations could be induced by UV (*i.e.*, 337 nm),[19] and that DNA damage was dramatically decreased above 470 nm.[20] Furthermore, recent studies have demonstrated that UV light could directly induce alterations in the DNA, and lead to immunosuppression *in vivo*.[21,22] In another study, Fedorovich *et al.* demonstrated that the combination of UV light and the photoinitiator Irgacure 2959 resulted in harmful effects on cell viability.[23] However, it was shown that the photopolymerization process in the presence of hydrogel precursors led to higher cell viability. This observation suggested that free radicals generated through photopolymerization were consumed during the crosslinking process, reducing the damage to cellular components.[23] These studies taken together demonstrated that the combination of visible light with safer photoinitiators as the energy source for the crosslinking reaction, can enhance the utility of photocrosslinkable hydrogels for tissue engineering applications. Additionally, visible light has been shown to penetrate tissues at higher depths and with lower energy, as compared to UV light.[24] This characteristic makes visible light suitable for developing *in situ* injectable materials, for minimally invasive procedures.

Eosin Y is a Food and Drug Administration (FDA)-approved photoinitiator excited by visible light (450–550 nm) (Fig. 1a and b), which was used in the photocrosslinkable lung sealant FocalSeal® (Genzyme Biosurgical, Cambridge, MA). Eosin Y has been used in many thiol–ene crosslinking reactions to fabricate hydrogel-coated surfaces,[25] cell-laden hydrogels,[26] and growth factor delivery systems.[27] Other photoinitiators such as camphorquinone, fluorescein, and riboflavin have also been used to initiate photocrosslinking upon exposure to blue light.[18] However, the use of prolonged irradiation to

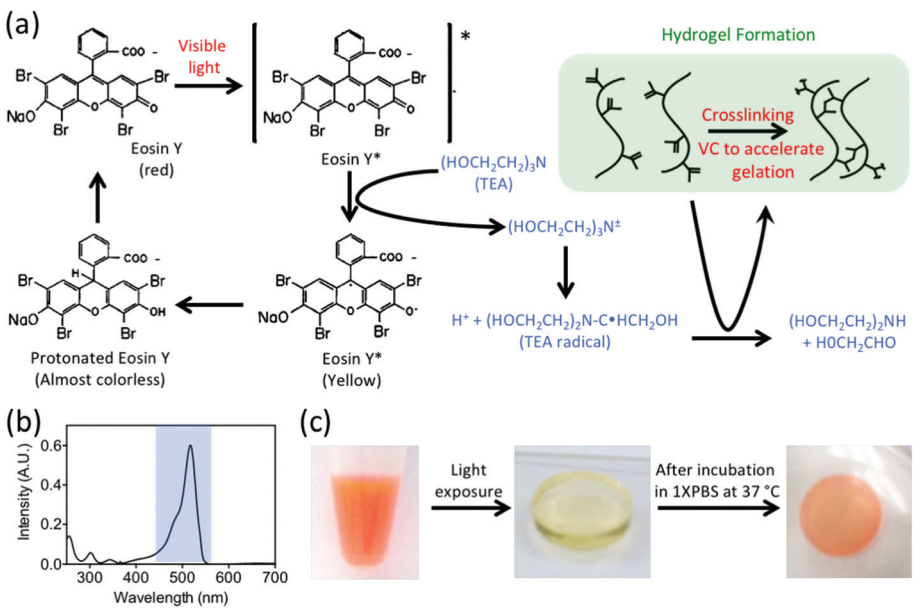

Fig. 1 The Eosin Y-based photopolymerization system. (a) A schematic representation of radical generation reactions initiated by photo-induced activation of Eosin Y. (b) UV-vis spectra of Eosin Y at pH 7.4. (c) Visualization of the color change during the hydrogel formation, indicating the activated state of Eosin Y.

obtain hydrogels with an appropriate mechanical strength with these photoinitiators may lead to toxic effects on the encapsulated cells, when using them as cell-laden hydrogels.[28]

Several groups have reported the application of injectable hydrogels for cardiac tissue regeneration. For example, an ECM-derived hydrogel was used as an injectable material for the treatment of infarcted myocardial tissue.[29] The injection of this hydrogel into infarcted pig hearts led to increased cell infiltration due to tissue self-assembly into the porous scaffold. In addition, histological analysis showed that a layer of endocardium was developed due to the injection of the hydrogel.[29] Other studies reported the use of UV light crosslinkable hydrogels for the repair of anterolateral cardiac incisions. These results showed an increase in wall thickness of the left ventricle, which enhanced the survival of both viable and infarcted cardiac tissues.[30–32]

Here, we report the synthesis of a gelatin-based hydrogel for myocardial repair *via* visible-light-initiated photocrosslinking, using Eosin Y as a photoinitiator, triethanolamine (TEA) as a co-initiator and *N*-vinylcaprolactam (VC) as a co-monomer. The GelMA prepolymer solution was photopolymerized upon exposure to visible light to form hydrogels with tunable physical properties. We evaluated the mechanical properties, porosity, and swelling behavior of the engineered hydrogels, as well as their *in vitro* and *in vivo* biocompatibility. We also investigated the feasibility of hydrogel delivery to infarcted hearts *in vivo*. It is hypothesized that the engineered material can be used as a safe and fast polymerizable hydrogel with controlled physical properties. In addition, they could also be used for the repair of a variety of soft tissues such as heart, blood vessels, and skin, and may facilitate the clinical translation of injectable hydrogels for soft tissue regeneration.

Results and discussion

In this study, we engineered injectable visible light crosslinked GelMA hydrogels for cardiac tissue repair. These hydrogels were formed by the photochemical reaction of methacryloyl units, available on GelMA chains and activated by Eosin Y, which absorbs light between 450 and 550 nm (Fig. 1a and b).[1,3] Photocrosslinking *via* UV light (250 nm < λ < 400 nm) relies on the use of photoinitiators such as Irgacure 2959.[26,27] However, alternative photoinitiators such as VA-086 that absorb safer UV ranges (≈405 nm) than Irgacure 2959 and lead to enhanced cytocompatibility have recently been described.[33] UV light photons cause dissociation of the photoinitiator into two radicals, which cause radical formation on the methacryloyl groups. Since radicals are unstable entities, they quickly combine with each other in their vicinity, leading to a crosslinked network. An alternative to UV photoinitiation is using Eosin Y in combination with visible light (400 nm < λ < 700 nm). Visible light excites Eosin Y from the ground state into a triplet state. This then extracts hydrogen atoms from amine-functionalized co-initiators, such as TEA. The deprotonated TEA radical then initiates the formation of a radical center on the methacryloyl groups of GelMA. Visible light mediated polymerization often requires co-monomers, such as VC, to generate an adequate number of radicals to accelerate the gelation process (Fig. 1).[34] This increased gelation rate in the presence of VC could be due to an increased vinyl group concentration, and/or rapid diffusion of radicals bearing VC.[26] In addition, photoinitiation *via* Eosin Y could be visually confirmed by a change in color from red to yellow, which occurs after the formation of activated Eosin Y (Fig. 1c).

It has been reported that in an ideal and fully crosslinked hydrogel network with a certain prepolymer molecular weight and functionality, the crosslinking density of the hydrogel should not be affected by the photoinitiator and co-initiator concentrations.[35] Therefore, the physical properties of the hydrogel, such as pore characteristics, swelling ratios, and mechanical properties, should also remain constant. However, in a visible light system, which is based on free radical chain reaction polymerization, an ideal fully crosslinked hydrogel network cannot be obtained due to the presence of unreacted functionalities, dangling polymers, and primary cycles.[35] This behavior is particularly observed at lower prepolymer or initiator concentrations.[36] Therefore, in our system, since the hydrogel network was not fully crosslinked even after 180 s light exposure, the physical properties of the engineered hydrogels were dependent on TEA, Eosin Y, and VC concentrations.

Previous studies have investigated the effects of photoinitiator and co-initiator concentrations on the physical properties of visible light crosslinked hydrogels.[25,26,36,37] For example, Bahney *et al.* investigated the effect of Eosin Y (0.001–0.1 mM) and TEA (0.01–1.5%) concentrations on the mechanical properties of visible light crosslinked poly(ethylene glycol) diacrylate (PEGDA) hydrogels.[37] Their results demonstrated that the dynamic modulus of the resulting PEGDA hydrogels ranged from 25 to 125 kPa at 120 s light exposure time.[37] In another study, Shih *et al.* also showed that by increasing the Eosin Y concentration from 0.1 to 2.0 mM, the swelling ratio of a visible light crosslinked PEG-based hydrogel increased approximately 2-fold at 240 s light exposure time.[25] Here, we investigated the effects of these variables on the physical properties (*i.e.*, porosity and swellability) of the engineered GelMA hydrogels (Fig. 2). The porosity of a hydrogel is key for its interaction with cells and the surrounding tissues.[2,38–40] The modulation of the micro-architectural properties and the porosity of a hydrogel could be used to deliver bioactive cues to cells growing within the engineered constructs.[2,39] Additionally, increased porosity promotes cellular penetration and new tissue formation within the 3D structure of the hydrogels.[2] For these experiments, we used a fixed concentration of 0.1 mM Eosin Y. Eosin Y regenerates during light exposure, whereas TEA radicals and VC are consumed by the crosslinking of GelMA, as shown in Fig. 1a. Therefore, we anticipated that the swelling ratio and pore size are more dependent on the concentration of TEA and VC than Eosin Y. Our results demonstrated that the apparent pore size in the

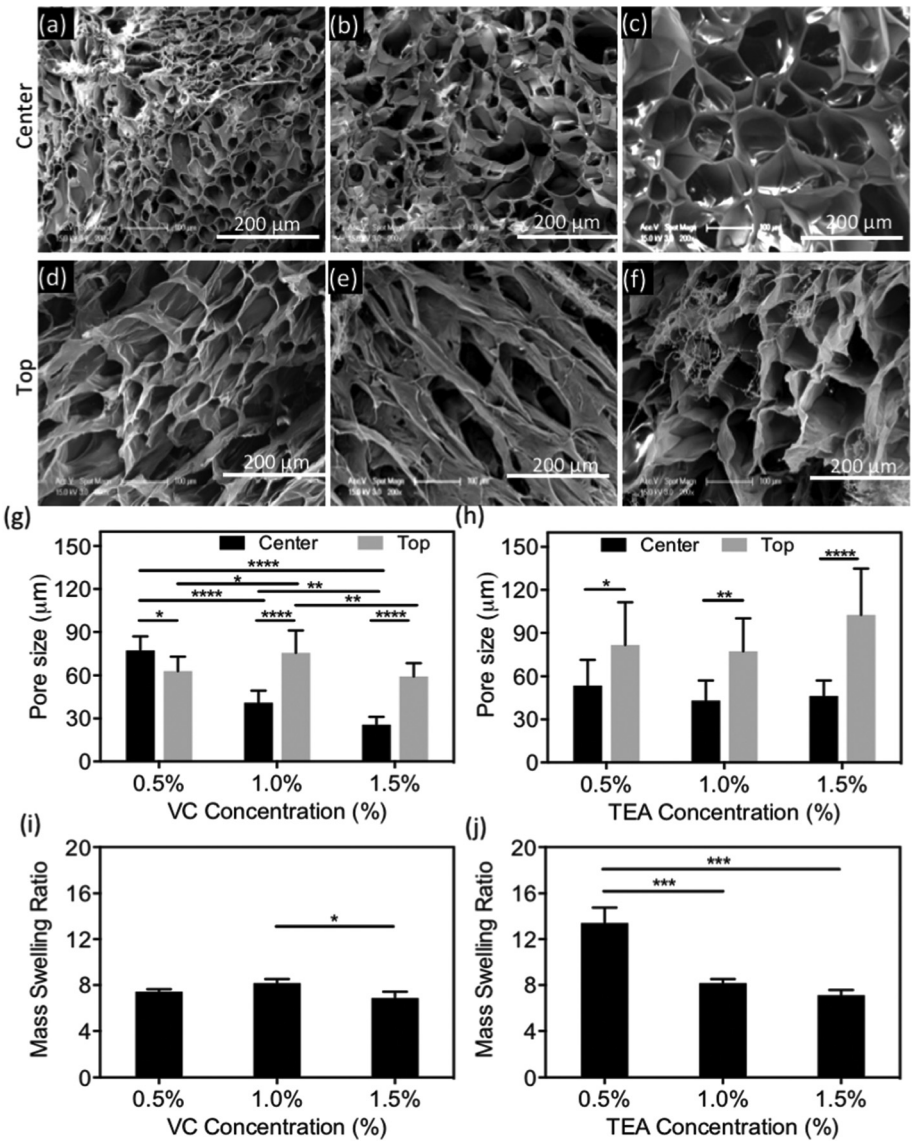

Fig. 2 Porosity and swelling properties of visible light crosslinked GelMA hydrogels. (a–f) Representative SEM images of 10% (w/v) GelMA hydrogels made with 1% (w/v) TEA and 0.1 mM Eosin Y and 180 s light exposure time, at a distance of 1 cm with (a, d) 1.5, (b, e) 1.0, and (c, f) 0.5% (w/v) VC concentrations. Paired images (center/top) were acquired from the same hydrogels (scale bars: 200 μm). Effect of (g) VC and (h) TEA concentrations on the average pore sizes measured from SEM images. Error bars represent the SD of measurements on 3 different positions in 3 independent SEM images of each hydrogel (*$p < 0.05$, **$p < 0.01$, ***$p < 0.001$ and ****$p < 0.0001$). The effect of (i) VC (1% (w/v) TEA) and (j) TEA concentrations (1% (w/v) VC) on the swelling ratio of GelMA gels produced using 10% GelMA and 0.1 mM Eosin Y.

central area of GelMA hydrogels decreased from 77.1 ± 9.9 μm to 41.0 ± 8.4 μm and 25.6 ± 5.5 μm as the VC concentration increased from 0.5% (w/v) to 1% (w/v) and 1.5% (w/v), respectively, for hydrogels with 10% (w/v) GelMA, 1% (w/v) TEA, and 0.1 mM Eosin Y (Fig. 2a–c and g). We also investigated the changes in hydrogel porosity caused by varying the concentration of TEA (Fig. S1† and Fig. 2h). However, we did not observe any statistically significant differences in pore size between hydrogels produced by using different TEA concentrations. Similarly, the pore sizes on the surface of the hydrogels could also be tuned by varying the concentration of VC (Fig. 2g). It is important to note that the apparent porosity of the hydrogel could be due to lyophilization of the hydrogels prior to SEM analysis. Previous studies have shown that the pore size of hydrogels could be affected by the freezing temperature before lyophilization.[2] In our study, all samples were processed following a methodology reported previously to compare the average pore size through SEM analysis, using different formulations of UV crosslinked GelMA hydrogels.[15] In general, GelMA hydrogels crosslinked *via* visible light showed a pore size distribution similar to that of UV crosslinked GelMA hydrogels. The effects of VC and TEA concentrations on the maximum swelling ratio of the engineered hydrogels were also investigated (Fig. 2i–j). As shown in Fig. 2i,

the swelling ratio decreased significantly from 8.2 ± 0.36% to 6.9 ± 0.55% when the concentration of VC increased from 1.0% (w/v) to 1.5% (w/v). In addition, increasing TEA concentrations from 0.5% (w/v) to 1.0% (w/v), and 1.5% (w/v) reduced the swelling ratios from 13.4 ± 1% to 8.2 ± 0.3% and 7.1 ± 0.4%, respectively (Fig. 2j). For all these hydrogels, 10% (w/v) GelMA and 0.1 mM Eosin Y were used. These results suggested that lowering the concentration of the co-initiator and the co-monomer may also lower the crosslinking density and lead to a higher swelling capacity.

The mechanical properties of photocrosslinked GelMA hydrogels were also tuned by changing the concentrations of TEA and VC (Fig. 3). Our results showed that GelMA hydrogels exhibited tunable compressive moduli in the range of 5–56.5 kPa, and tensile moduli ranging from 5 to 22.7 kPa, depending on the VC and TEA (Fig. 3). The compressive moduli of 10% (w/v) GelMA hydrogels, formed by using 1.0% (w/v) TEA, and 0.1 mM Eosin Y, decreased from 26.9 ± 9.9 kPa to 17.2 ± 5.7 kPa and 10.3 ± 5.2 kPa when the VC concentrations were lowered from 1.5% (w/v) to 1% (w/v) and 0.5% (w/v), respectively (Fig. 3a–c). In addition, the tensile moduli of the hydrogels decreased from 15.1 ± 4.0 kPa to 12.9 ± 1.7 kPa and 6.3 ± 0.6 kPa when the VC concentrations were lowered from 1.5% (w/v) to 1% (w/v) and 0.5% (w/v), respectively, at a constant 1.0% (w/v) TEA and 0.1 mM Eosin Y concentration (Fig. 3d–f). Increasing the VC and TEA concentrations influences the dynamics of the reaction, and thus, the number of crosslinking sites may increase at a constant light exposure time (*i.e.*, 180 s). This enhanced crosslinking density may result in an increase in hydrogel stiffness, as well as a decrease in the swelling ratio and pore sizes.[34] These results are in agreement with our previous work based on engineering of UV light crosslinked GelMA and methacryloyl-substituted tropoelastin (MeTro) hydrogels.[9,15] In this study, the mechanical properties of the hydrogels were dependent on the prepolymer and initiator concentrations, as well as light exposure time. We also investigated the effect of varying the concentration of Eosin Y on the mechanical properties of the engineered GelMA hydrogels. Our results showed that the highest compressive modulus was obtained at 0.1 mM Eosin Y for 10% GelMA hydrogels with 1% (w/v) VC and 1% (w/v) TEA (Fig. S2†). The mechanical properties of the engineered GelMA hydrogels (6–56.5 kPa) in this study were in the range of those reported previously for UV crosslinked GelMA hydrogels (5–50 kPa).[15] In addition, the mechanical strength was comparable to that of native heart tissue (*i.e.*, Young's modulus: 10–50 kPa).[41,42] These observations suggest that GelMA hydrogels should integrate well with native tissue, without causing failure due to the mechanical mismatch. Based on the mechanical characterization, the optimized hydrogel formulation of 10% (w/v) GelMA, 1.5% (w/v) TEA, 1% (w/v) VC and 0.1 mM Eosin Y was used for all *in vitro*, *ex vivo* and *in vivo* experiments. In particular, the light exposure time (*i.e.*, 180 s) for hydrogels with 1 mm thickness synthesized for mechanical characterization, *ex vivo* and *in vivo* experiments was lowered to 20 s for the 150 μm-thick hydrogels used in *in vitro* experiments.

Engineering of cardiac tissue constructs requires a matrix/scaffold for the maintenance of cell viability, organization, and tissue formation.[27] Therefore, we investigated the suitability of the engineered visible light crosslinked GelMA hydrogel as a matrix to support cardiomyocyte (CM) growth. We first investigated the *in vitro* cytocompatibility of GelMA hydrogels using surface seeding (2D, Fig. S3a–f†) and 3D encapsulation (Fig. S3g–l†) of NIH 3T3 fibroblasts. We used a standard live/dead assay to calculate cell viability, by determining the percentage of live cells seeded in 2D (Fig. S3c†) and 3D (Fig. S3i†) cultures with respect to total cells. These results demonstrated that cell viability remained >90% for both 2D and 3D cultures. In addition, fibroblasts grown in both 2D (Fig. S3d–f†) and 3D (Fig. S3j and k†) cultures could spread and proliferate for up to

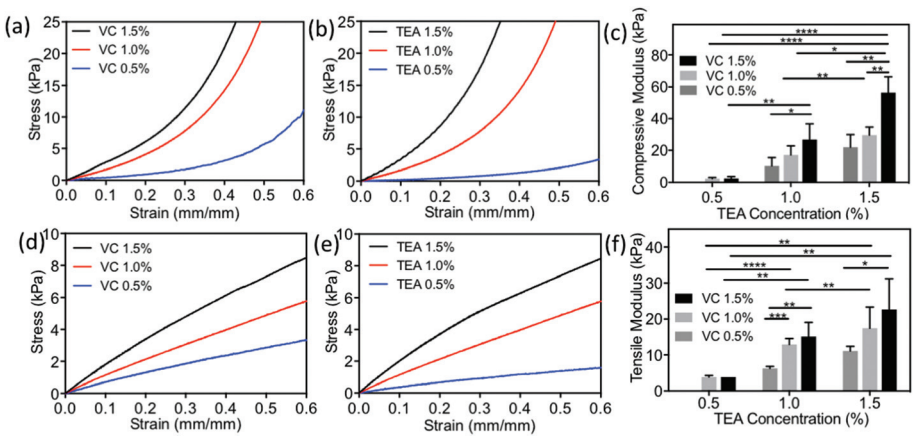

Fig. 3 Mechanical properties of visible light crosslinked GelMA hydrogels. (a, b) Representative compressive strain/stress curves and (c) compressive modulus of 10% (w/v) GelMA hydrogels made at various concentrations of TEA and VC with 0.1 mM of Eosin Y at 180 s light exposure time, at a distance of 1 cm. (d–e) Representative tensile strain/stress curves and (f) tensile modulus of GelMA hydrogels produced at various concentrations of TEA and VC with 0.1 mM of Eosin Y. Error bars represent the SD of measurements on 3 independent samples (*$p < 0.05$, **$p < 0.01$, ***$p < 0.001$ and ****$p < 0.0001$).

7 days as confirmed by nuclei and F-actin staining. These results demonstrated that visible light crosslinked hydrogels could efficiently support the growth, spread, and proliferation of NIH 3T3 fibroblasts grown in both 2D and 3D cultures. We then evaluated the ability of the engineered GelMA hydrogels to support the growth and contractile function of primary rat CMs *in vitro*. We have previously shown that UV crosslinked GelMA hydrogels could be used to engineer cardiac tissue constructs.[11,43] Although these GelMA-based hydrogels were shown to support the growth of CMs *in vitro*, direct *in vivo* delivery could potentially impair cardiac function due to tissue damage caused by UV light. Therefore, we aimed at addressing this limitation by using visible light to form a highly biocompatible cell-laden hydrogel that could preserve the contractile function of CMs. For these experiments, we also used a live/dead assay and DAPI/F-actin staining to evaluate cell viability (Fig. 4a–d) and spread (Fig. 4e–h) of CMs on the engineered GelMA hydrogels. Our results demonstrated that the viability (Fig. 4d) and the number of cells on the surface of GelMA hydrogels (Fig. 4h) increased significantly at day 5, compared to day 1 post seeding. In particular, the cell number on GelMA hydrogels increased from 92 cells per mm^2 on day 1 to 205 cells per mm^2 on day 5 (Fig. 4h). However, this observation could be due to the proliferation of cardiac fibroblasts that could not be removed after CM isolation.

Previous studies have demonstrated that CMs maintained under conventional 2D culture conditions tend to regress to a less mature phenotype, and lose the ability to respond to physiological stimuli.[44,45] Thus, we investigated the ability of GelMA hydrogels to maintain the phenotype of primary rat CMs *in vitro*. First, we evaluated the expression of the CM marker sarcomeric α-actinin (SAA) using 2D cultures of primary CMs on GelMA hydrogels. Our results showed positive immunolocalization of SAA in CMs maintained on the engineered GelMA hydrogels after 7 days of culture (Fig. 4i). In addition, fluorescent images showed that cells exhibited well-defined, cross-striated sarcomeric structures, which resembled those of the native rat ventricular myocardium[46] (Fig. 4i). Lastly, we evaluated the ability of visible light crosslinked GelMA hydrogels to support the contractile function of primary CMs growing on 2D cultures. These results showed that CMs exhibited synchronous contractions when cultured on the surface of GelMA hydrogels (ESI,† Videos 1 and 2). The beating frequency of CMs was quantified up to 10 days after seeding, and was shown to vary from 18 to 77 beats per min (Fig. 4j). Furthermore, the metabolic activity of cardiac cells on

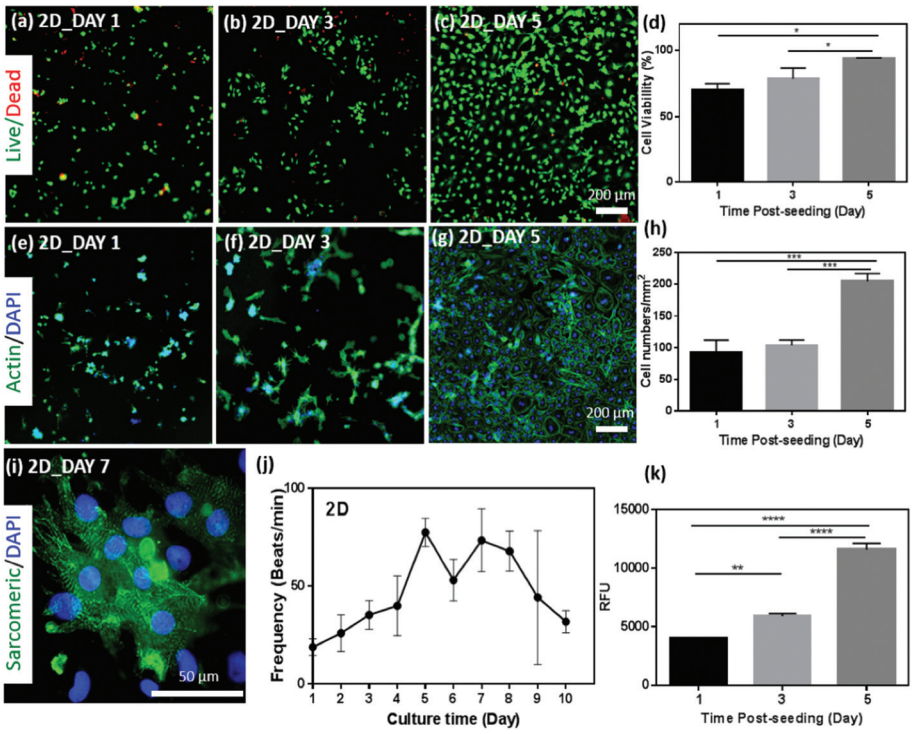

Fig. 4 *In vitro* 2D seeding of CMs on visible light crosslinked GelMA hydrogels (GelMA concentration: 10% (w/v), TEA: 1.5% (w/v), VC: 1% (w/v), and 0.1 mM Eosin Y). (a–c) Representative live/dead images of CMs seeded on the surface of the hydrogels on days 1, 3, and 5. (d) Quantification of CM viability cultured on the GelMA hydrogels after 1, 3, and 5 days of culture (scale bars: 200 μm). (e–g) Representative F-actin/DAPI stained images of CMs seeded on GelMA hydrogels after 1, 3, and 5 days of seeding (scale bar = 200 μm). (h) Cell proliferation on the hydrogels after 1, 3, and 5 days of seeding, quantified from F-actin/cell nuclei stained images. (i) Immunostaining for the expression of sarcomeric α-actinin (green)/DAPI (blue) on day 7 of culture (scale bar = 50 μm). (j) Beating characterization of CMs cultured on the surface of the hydrogel. (k) Quantification of the metabolic activity of CMs using PrestoBlue assay 1, 3, and 5 days after seeding (RFU: relative fluorescence intensity) (*$p < 0.05$, **$p < 0.01$, ***$p < 0.001$ and ****$p < 0.0001$).

2D cultures increased significantly at day 5 post seeding, as shown by a commercial PrestoBlue assay (Fig. 4k). Taken together, these results demonstrated that visible light crosslinked GelMA hydrogels could be used to support the growth and preserve the contractile function and phenotype of primary CMs *in vitro*.

We then performed *ex vivo* tests to investigate the injectability of GelMA hydrogels, and the possibility to photopolymerize the gels with visible light following injection into the myocardium (Fig. 5). For this, 200 μL of GelMA prepolymer (10% (w/v)) was injected into the right ventricle of an excised, adult Sprague–Dawley rat heart, followed by 180 s of exposure to visible light, at a distance of 1 cm. The presence of the photocrosslinked hydrogels within the explanted tissue was then verified *via* immunofluorescence staining (nuclei – DAPI; α-smooth muscle actin (αSMA) – TRITC) of cryosectioned right ventricular tissue. Due to the strong auto-fluorescence of Eosin Y,[47,48] the engineered hydrogels appeared as large green fluorescent areas devoid of nuclear staining, which suggested that GelMA was successfully injected into the myocardium and was photocrosslinked *in situ* (Fig. 5a–d). In addition to the lack of cellularity, the structure and morphology of the injected GelMA is vastly different from that of healthy tissue (Fig. 5a–d). Furthermore, the positive green fluorescence within the αSMA positive vascular structures suggested that GelMA was crosslinked within the blood vessels (Fig. 5c). However, this was mainly because the injection was performed *ex vivo*, where the absence of blood flow allowed for the infiltration of small amounts of hydrogel precursor into the vasculature. The presence of GelMA hydrogels within the ventricular wall was further confirmed through H&E staining of tissue cryosections following *ex vivo* injection (Fig. 5e–h). Histological assessment revealed acellular regions with increased matrix density, as compared to the surrounding healthy myocardium (Fig. 5e–h). These results confirmed that visible light crosslinked GelMA materials can be injected and photocrosslinked *in situ*, demonstrating their suitability for cardiac tissue engineering applications.

Next, we aimed at investigating the regenerative potential and *in vivo* injectability of visible light crosslinked GelMA hydrogels using a myocardial infarction (MI) model. MI was induced in 8-week-old Sprague–Dawley rats *via* permanent ligation of the coronary artery. Next, 50 μL of the prepolymer solution (10% (w/v)) was injected into 4 areas (200 μL in total) within the infarcted region of the left ventricle, followed by photocrosslinking by exposure to visible light for 180 s, at a distance of 1 cm (Fig. 6a and b). Animals receiving saline injections (sham) were used as controls (Fig. 6c and e). The efficient delivery of GelMA hydrogels *in vivo* following MI demonstrated the feasibility for injection and *in situ* gelation during open-heart surgeries (Fig. 6d and f). Crosslinked GelMA was visible from the epicardial surface (Fig. 6d) and was also visible as a change in ECM density in Masson's trichrome images of hearts isolated immediately post injection (Fig. 6f). Animals were sacrificed 3 weeks after MI, and cardiac tissues were harvested and processed for histological

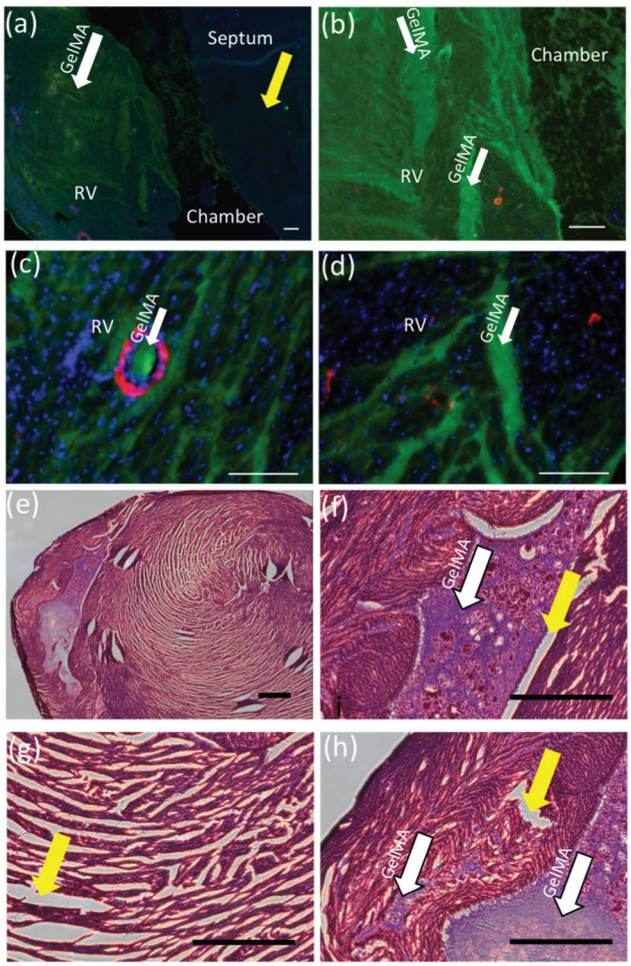

Fig. 5 *Ex vivo* evaluation of injectability and *in situ* polymerization of visible light crosslinked GelMA hydrogels. (a–d) Immunofluorescence staining of the right ventricular cardiac muscle cryosections following injection and polymerization. GelMA could be visualized due to the strong green autofluorescence of the eosin Y-containing hydrogels, in the absence of nuclear staining (DAPI, blue). The adjacent unstained myocardium is identified with a yellow arrow. The presence of GelMA hydrogels within the αSMA stained (TRITC, red) vasculature is indicated by a white arrow (scale bar = 100 μm). (e–h) Hematoxylin and eosin (H&E) staining of the cryosectioned myocardium showing the injected GelMA hydrogels (white arrows). The GelMA injection into the explanted myocardium led to an increase in matrix density with obvious differences in architecture. The myocardium in the absence of GelMA shows a distinct architecture void of the areas with high matrix content, as noted by yellow arrows (scale bar = 500 μm). Hydrogels were prepared using 10% (w/v) GelMA, 1.5% (w/v) TEA, 1% (w/v) VC, 0.1 mM Eosin Y, and 180 s light exposure time, at a distance of 1 cm.

assessment. As expected, the scar tissue on the free wall from the left ventricles of animals upon MI became thin and collagenous, with few histological differences among the infarcted groups, as demonstrated by Masson's trichrome staining (Fig. 6g–i).

Differences were apparent upon GelMA treatment in the immunofluorescence staining of the infarct region of the hearts. Due to the permanent ligation of the left coronary

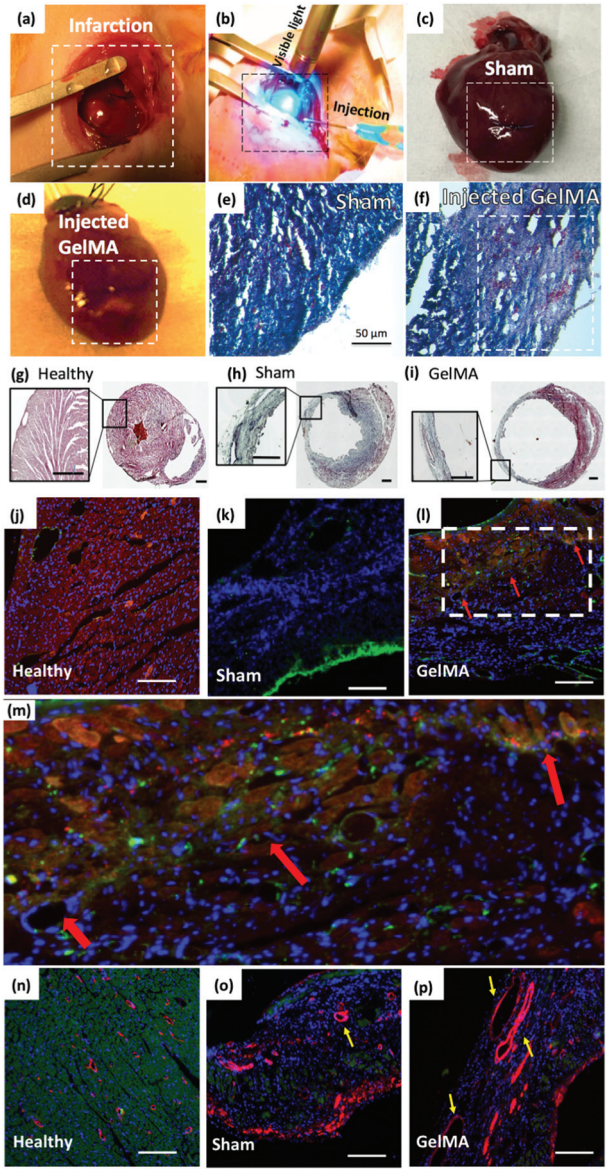

Fig. 6 *In vivo* injection and polymerization of visible light crosslinked GelMA hydrogels. (a–d) Representative images showing: (a) the ligature of the coronary in the left ventricle to induce the infarct, (b) the delivery and *in situ* photocrosslinking of GelMA hydrogels, (c) excised heart with injected saline (sham), (d) excised heart with injected visible light crosslinked GelMA hydrogels. (e, f) Masson's trichrome staining of the hearts immediately post injection. GelMA presence is detected as a color change shown within the dotted yellow box. Histological assessment (Masson's trichrome) of cryosectioned explanted myocardium samples from (g) healthy, (h) sham, and (i) GelMA-treated animals (scale bars = 1 mm). Immunofluorescence staining of cryosectioned explanted myocardium samples from (j) healthy, (k) sham, and (l) GelMA-treated animals, against cardiomyocytes/cardiac α-actin (CAA, TRITC, red) and endothelial cells (von Willebrand factor (vWF), GFP, green) 3 weeks post myocardial infarction (MI). (m) Increased magnification of the dotted area in panel (l), showing increased CM (red arrows) density (scale bars = 50 μm). Immunofluorescence staining against myosin heavy chain (MHC, GFP, green) and α-smooth muscle actin (αSMA, TRITC, red) in cryosectioned samples from (n) healthy, (o) sham, and (p) GelMA-treated animals. αSMA staining coincides with large vessels (yellow arrows) (scale bars = 50 μm). Hydrogels were synthesized using 10% (w/v) GelMA, 1.5% (w/v) TEA, 1% (w/v) VC, and 0.1 mM Eosin Y.

artery, significant decreases in cardiac α-actin (CAA)+ CMs were observed in the left ventricle of the sham and GelMA treated animals after 3 weeks (Fig. 6j–m). However, small numbers of CAA+ CMs and von Willebrand factor (vWF)+ endothelial cells were identified in the inner region of the scar area in GelMA treated animals (Fig. 6l and m). This observation suggested that the GelMA injection may alter the rate of remodeling of the damaged tissue, given that the sham did not show any positive staining for SAA. In addition, positive staining for vWF was only observed in the endothelium lining the inner ventricular surface (Fig. 6k). Typically, the infarct region becomes inundated with activated cardiac fibroblasts (also called myofibroblasts), which are defined by the expression of αSMA. The reduction in αSMA+ cells within the GelMA treated scar region, as compared to the sham scar region, suggested a reduction in myofibroblast activation 3 weeks after MI (Fig. 6n and o). αSMA expression in GelMA treated tissues more closely resembles that of healthy tissues, with no positive αSMA staining outside of the vessel linings. In addition, our results also showed the maintenance of larger vessels normally present in healthy tissue, as opposed to smaller neo-vessels present in the remodeled infarcted region in control (sham) animals (Fig. 6n–p). Therefore, the delivery of GelMA hydrogels appeared to enhance CM viability, which might be due to the modulation of the remodeling response of the tissue (evidenced by reduced αSMA+ fibroblasts), as well as the maintenance of larger vessels in the infarcted region (Fig. 6p). However, further studies are necessary to fully determine the exact nature of these effects. Previous studies have demonstrated that upon MI, cardiac stem cells (CSCs) migrate to the site of injury and participate in the repair of the injured tissue.[49,50] In addition, we have also demonstrated previously that UV crosslinked GelMA-based hydrogels could support capillary formation *in vivo* after implantation[14] and after injection.[51] Therefore, GelMA hydrogels could potentially be used to support the homing and attachment of migratory CSCs and to promote vascularization *in vivo*, which would potentially promote regeneration after MI.

In summary, we demonstrated the possibility to photocrosslink GelMA hydrogels *in situ* using visible light, following intramyocardial delivery. *In vivo* studies following MI confirmed that the delivery of photocrosslinkable GelMA hydrogels appears to be safe and feasible. However, more comprehensive experiments should be undertaken to optimize the delivery of the hydrogels and to assess the potential benefits of GelMA hydrogels in improving cardiac function after MI.

Conclusion

Here, we have developed visible light crosslinked GelMA hydrogels with tunable physical properties. The use of visible light may help circumvent the potential biosafety concerns associated with the use of toxic initiators or UV light. The physical properties of the engineered hydrogels (*i.e.*, mechanics, swelling behavior, and porosity) could be modulated by varying the

concentrations of the photoinitiators in the hydrogel precursor solution. For example, the compressive modulus could be tuned in the range of 5–56.5 kPa, making it a suitable candidate for soft tissue engineering applications. In addition, the engineered hydrogels were shown to be cytocompatible, both *in vitro* and *in vivo*. The safe delivery and *in situ* polymerization of visible light crosslinked GelMA hydrogels make them remarkably suitable for tissue engineering applications and lithography-based platforms, where the use of UV light may potentially affect biological functions.

Experimental

Synthesis of gelatin methacryloyl (GelMA)

GelMA was synthesized as described previously.[15] Briefly, 10 g of gelatin (Sigma-Aldrich, from porcine skin) was dissolved in 100 mL of Dulbecco's phosphate buffered saline (DPBS) (Gibco®) at 50 °C. 8 mL of methacrylic anhydride (MA, Sigma-Aldrich) was slowly added dropwise to the gelatin solution at 50 °C under vigorous stirring, and then the mixture was kept for 3 h at 50 °C. After a two-fold dilution with DPBS (pre-warmed at 50 °C), the solution was dialyzed against distilled water by using a dialysis membrane (Spectrum® Laboratories, MWCO = 12–14 kDa) for 7 days at 40 °C, followed by lyophilization.

Preparation of GelMA hydrogels

A 12.5% (w/v) GelMA solution was prepared in DPBS containing 1.875% (w/v) of triethanolamine (TEA, Sigma Aldrich) and 1.25% (w/v) of *N*-vinylcaprolactam (VC, Sigma Aldrich) at 40 °C. Eosin Y was separately dissolved in fresh DPBS at a concentration of 0.5 mM. To prepare the hydrogel, 8 μL of GelMA solution was mixed with 2 μL of Eosin Y solution, and then the mixture was put between two glass coverslips separated by 150 μm spacers, followed by exposure to blue-green light (100 mW cm^{-2}, a xenon source from Genzyme Biosurgery) in the range of 450 to 550 nm. The final concentration of chemicals after forming the hydrogel was 10% (w/v) GelMA with 1.5% (w/v) TEA, 1% (w/v) VC, and 0.1 mM Eosin Y. GelMA solutions with various concentrations of TEA and VC (*e.g.* 0.625, 1.25, and 1.875% (w/v), referred to as the final concentrations: 0.5, 1.0, and 1.5% (w/v), respectively) were used to investigate the correlation between the concentration of chemical components and the mechanical strength of the hydrogel. Blue-green light (100 mW cm^{-2}, a xenon source from Genzyme Biosurgery) in the range of 450 to 550 nm was used to crosslink the hydrogels.

Swelling ratio measurements

The equilibrium swelling ratios of GelMA hydrogels were determined at 37 °C in DPBS. GelMA hydrogels for evaluating the swelling behavior were prepared in a cylinder-shaped polydimethylsiloxane (PDMS) mold (7 mm in diameter, 1 mm in depth). 80 μL of the precursor solution were exposed to blue-green light for 180 s, at a distance of 1 cm, in a mold covered with a glass coverslip. The formed hydrogels were removed from the mold and detached from the glass coverslip, followed by washing with DPBS for 5 min. The samples were lyophilized, and then their weights in the dried state were measured. Their mass values were measured again after incubating in DPBS for 24 h. The swelling ratio was defined as the ratio of the mass value after swelling to the mass value of dried samples after lyophilization.

Scanning electron microscopy (SEM) analysis

SEM analysis was performed to evaluate the porosity of the crosslinked hydrogels. Samples were frozen at −70 °C overnight and then dried under vacuum overnight. Lyophilized samples were prepared as described above for swelling ratio measurements. SEM images were obtained using a FEI/Phillips XL30 FEG SEM (15 kV), and lyophilized gels were coated with gold prior to analysis. The pore sizes of GelMA gels were averaged from at least 3 images from 3 samples for each condition (n = 100).

Mechanical characterization

The tensile and compressive strengths of GelMA hydrogels were measured using an Instron 5542 mechanical testing machine with a 10 N loading cell. For compression tests, GelMA hydrogels were prepared in the same way as that described above for swelling ratio measurements. After light exposure, the crosslinked hydrogels were incubated in DPBS for 1 h, and then the size of swollen gels was measured using a digital caliper l (diameter: 7.5 ± 0.12 mm, thickness: 1.5 ± 0.10 mm) prior to testing. Compression tests were performed at 1 mm min^{-1} speed until failure. The compressive modulus was calculated as the tangent slope of the linear region (0% to 5% strain) of the stress–strain curves. For tensile tests, hydrogels were prepared in rectangular molds (length: 8.9 ± 0.13 mm, thickness: 1.7 ± 0.10 mm, and width: 4.6 ± 0.15 mm). The hydrogels were allowed to swell for 1 h in DPBS before measurements. Then, both edges of the hydrogels were attached to fine adhesive tape and placed on the grips of the machine. The measurements were performed at 2 mm min^{-1} speed until failure occurred. The elastic modulus was calculated as the tangent slope of the linear region (0% to 5% strain) of the stress/strain curves. Three samples were tested for each condition.

Cell isolation and culture

Primary rat CMs were isolated from 2-day-old neonatal Sprague–Dawley rats by following the protocol approved by the Institute's Committee on Animal Care. Briefly, Sprague–Dawley neonatal pups were transferred into a clean cage and narcosis was induced using compressed CO_2. The pups were quickly decapitated with scissors after disinfecting the neck and sternum with 70% ethanol. The thorax was then opened through a straight line on the sternum to excise the heart. The isolated hearts were placed in cold Hank's Balanced Salt Solution (HBSS) buffer before removing the atria and blood vessels. Each heart was quartered and incubated in a solution

of trypsin (0.06% (w/v)) in HBSS at 4 °C for 16 h on a shaker. Trypsin digestion was then stopped by adding culture medium, followed by shaking for 5 min at 37 °C. The tissues were then serially digested in collagenase type II solution (0.1% (w/v)) in HBSS (10 min incubation with shaking at 37 °C for each digestion). The supernatant from the first digestion was discarded, and the cell suspensions from the subsequent second to third digestions were centrifuged at 1000 rpm for 5 min. Cells were then re-suspended in DMEM containing 10% FBS and 2 mM L-glutamine. The cell suspension was transferred to a T-175 flask and incubated for 1 h to enrich for CMs (cardiac fibroblasts were attached to the flask, while CMs remained in the suspension). Each hydrogel was then seeded with 7.5×10^5 cells in a 24 well plate immediately after pre-plating and cultured in DMEM containing FBS (10%), L-glutamine (1%, Gibco®), and penicillin–streptomycin (100 units per ml) for up to 14 days. NIH 3T3 fibroblasts were cultured in DMEM with 10% of FBS and 1% of penicillin–streptomycin. Cells were passaged approximately 2–3 times per week, and the culture medium was changed every 2 days.

Surface seeding (2D culture)

Hydrogel precursors (10 μL) were exposed to blue-green light for 20 s, at a distance of 1 cm, covered by a glass slide coated with 3-(trimethoxysilyl) propyl methacrylate (TMSPMA, Sigma-Aldrich) and confined in 150 μm spacers. NIH 3T3 cells (5×10^4 cells per scaffold) and CMs (7.5×10^5 cells per scaffold) were seeded on top of the hydrogels attached to the TMSPMA-treated glass slides. UV light crosslinked GelMA hydrogels were synthesized using 0.5% (w/v) Irgacure 2959 as a photo-initiator and 20 s light exposure (6.9 mW cm^{-2}).

Cell encapsulation (3D culture)

NIH 3T3 cells were trypsinized and re-suspended (5×10^6 cells per mL) in the hydrogel precursor before light exposure. Cell-laden GelMA hydrogels (10 μL) were formed by exposure to blue-green light for 20 s, at a distance of 1 cm, and bound to TMSPMA-coated glass slides. The formed cell-laden gels were washed 3 times with DPBS and incubated in culture medium at 37 °C.

Cell viability

The viability of cells was measured using a LIVE/DEAD® Viability/Cytotoxicity kit for mammalian cells (Invitrogen™) according to the instructions from the manufacturer. Briefly, cells were stained with 0.5 μL mL^{-1} of calcein AM and 2 μL mL^{-1} of ethidium homodimer-1 (EthD-1) in DPBS for 15 min at 37 °C in the culture incubator. The stained cells (green for live cells, red for dead cells) were imaged using an inverted fluorescence microscope (Zeiss Axio Observer Z1) at 1, 4, and 7 days post seeding. The number of live and dead cells was quantified using the ImageJ software, and the viability was determined by the number of live cells divided by the total number of live and dead cells. Three samples were used per condition and three images were obtained from each sample to quantify cell viability.

Cell adhesion, proliferation and spreading

Cells were stained with rhodamine-phalloidin (Alexa Fluor 488-labeled or 594-labeled, Invitrogen™) and DAPI (4′,6-diamidino-2-phenylindole) (Sigma Aldrich) to image F-actin and cell nuclei of cells on the surface or within hydrogels cross-linked by visible light after 1, 4, and 7 days of seeding. For staining, cells were fixed in 4% (v/v) paraformaldehyde in DPBS (Sigma Aldrich) for 15 min, permeabilized in 0.1% (w/v) Triton X-100 (Sigma Aldrich) for 5 min, and then blocked in 1% (w/v) bovine serum albumin (BSA, Sigma Aldrich) for 30 min. F-actin was then stained using Alexa Fluor-488 phalloidin or Alexa Fluor-594 phalloidin (1 : 40 dilution) in 0.1% bovine serum albumin (BSA) in DPBS for 45 min. After F-actin staining, cells were incubated in 1 μL mL^{-1} DAPI in DPBS for 5 min to stain cell nuclei. Quantitative analysis of cell densities and cell spreading after 1, 4, and 7 days of seeding was performed using fluorescence images acquired using an inverted fluorescence microscope (Zeiss Axio Observer Z1). Cell density in 2D cultures was quantified using the number of DAPI-stained nuclei per given area. Cell spreading was quantified using positively stained F-actin per given area.

Immunostaining for cardiac markers

The expression of the cardiomyocyte marker sarcomeric α-actinin was analyzed by immunofluorescence staining after 7 days of 2D seeding following previously established protocols.[11] Briefly, cells on the gel were fixed in 4% paraformaldehyde for 1 h at room temperature and washed with DPBS, then permeabilized in 0.1% (w/v) Triton X-100 for 30 min, followed by blocking in 10% (v/v) goat serum in PBS containing 0.1% Triton X-100 for 1 h. Then, the cells were incubated with the primary antibody mouse-anti-sarcomeric α-actinin diluted at a 1 : 200 ratio in goat serum (10% (v/v)) overnight at 4 °C, with subsequent washing steps with DPBS. The samples were then incubated for 2 h at room temperature with the secondary antibody (Alexa Fluor 594 goat-anti-mouse) diluted in goat serum (10% (v/v), 1 : 200 ratio). After several washing steps with DPBS, the samples were stained with DAPI (1/1000 diluted in DPBS) for 5 min at room temperature. The stained gels were imaged using an inverted fluorescence microscope (Zeiss Axio Observer Z1) after washing 4 times with DPBS.

PrestoBlue assay

The metabolic activity of cells was measured on days 1, 3, and 5 using PrestoBlue assay (Life Technologies) according to the manufacturer's protocol. Briefly, samples were incubated with a solution containing 10% PrestoBlue reagent and 90% cell culture medium for an hour at 37 °C. The final fluorescence was measured using a BioTek UV/Vis Synergy HT microplate reader. The relative fluorescence values were calculated and reported for each day.

Ex vivo experiments

All animal studies were conducted in accordance with Tufts University Guidelines and with IACUC approval. For *ex vivo*

assessment of injectability into the myocardium, a male Sprague–Dawley rat (2+ months of age and 250–275 grams) was sacrificed *via* CO_2 asphyxiation followed by a thoracotomy. 200 μL of GelMA gel was injected into the free wall of the right ventricle and exposed to the visible light source for 180 s (100 mW m^{-2}) at a distance of 1 cm. The deformation of the right ventricle by the presence of a solid gel below the epicardium was apparent. The whole heart was subsequently processed for histological analysis as described below.

In vivo GelMA prepolymer injection and crosslinking

Male Sprague–Dawley rats (2+ months of age and 250–275 grams) were anesthetized with 4% isoflurane, and maintained at 2% during the surgery. Animals were intubated and received a thoracotomy between the 4^{th} and 5^{th} intercostal space. A retractor was placed between the ribs, the heart was exposed and an incision was made within the pericardium. A 6–0 prolene suture was used to permanently occlude the left coronary artery such that blanching occurred across 40% of the left ventricular free wall, based on our previously described procedure.[52] For the animals receiving the GelMA hydrogel injection (n = 3), 50 μL was delivered through a 25G needle to four distinct sites corresponding to the top center of the infarct, the leftmost edge of the infarct, the center of the infarct and the rightmost edge. After a total of 200 μL was delivered, the visible light source was turned on and positioned 2 cm away from the surface of the heart for 180 s, at a distance of 1 cm. Following light exposure, the lungs were fully inflated and the chest, muscle and skin were sutured closed. The animal was allowed to recover for 15 min under a heating lamp. The sham animals received the same surgical procedure, but were injected with 0.9% pharmaceutical-grade saline as opposed to the GelMA solution. Healthy animals did not undergo any surgical procedure, but were evaluated in the same manner as the other two experimental conditions. A total of 13 animals were used for the *in vivo* study with 2 healthy, 3 sham and 8 GelMA prepolymer injections. All animals survived the infarct and injection with no adverse events and were sacrificed 3 weeks after the surgery.

Heart isolation and histological assessment

Animals were sacrificed *via* CO_2 asphyxiation and hearts were isolated, fixed in 4% paraformaldehyde at 4 °C for 12 h and rinsed three times for 1 h in 1× DPBS. Hearts were immersed in 30% sucrose for 12 h, embedded in Optimal Cutting Temperature (OCT) compound and flash frozen by immersion in methyl butane that was chilled using liquid nitrogen. The frozen hearts were sectioned into 10 μm slices with a Cryotome E cryostat (Thermo Scientific, Waltham, MA). Masson's trichrome stain (Sigma Aldrich) was used to identify muscle (red) and collagen fibers (blue) by following the manufacturer's protocol. Images were acquired with a Leica DFC340 FX microscope (Wetzlar, Germany). Additional sections were rinsed in 1× DPBS and permeation was performed with 0.5% Triton X-100 solution for 5 min followed by three rinses for 5 min in 1× PBS. Samples were blocked in 1× PBS with 5% donkey serum and 1% BSA for 1 h at room temperature. Primary antibodies for myosin heavy chain (sc-32732, 1 : 100), cardiac α-actin (sc-58670, 1 : 100), smooth muscle α-actin (sc-32251, 1 : 200), and von Willebrand factor (Sigma F3520, 1 : 100) were diluted in 1% BSA. Cells were incubated in primary antibodies for 1 h at room temperature and then washed three times with 1× DPBS (incubation for 5 min each). Secondary antibodies (Alexa Fluor 488-conjugated donkey anti-rabbit A11008, Alexa Fluor 488-conjugated donkey-anti-goat A11055, and Alexa Fluor 555-conjugated donkey anti-mouse A31570) were diluted at 1 : 400 in 1% BSA in PBS. Cells were incubated with secondary antibodies with a 1 : 1000 dilution of a Hoechst fluorescent dye for 1 h at room temperature. Then, samples were washed with DPBS (3 × 5 min) and then imaged with an Olympus IX 81 fluorescent microscope.

Statistical analysis

Data were analyzed by one-way or two-way ANOVA followed by Tukey's *post-hoc* test (GraphPad Prism® 6.0c). Error bars represent the mean ± standard deviation (SD) of measurements ($^{*}p < 0.05$, $^{**}p < 0.01$, $^{***}p < 0.001$ and $^{****}p < 0.0001$).

Author contributions

Drs Annabi and Khademhosseini gave the idea of the project and helped with experimental design. Drs Noshadi and Hong assisted in the experimental design, and collected and analyzed the data for the materials characterization. E. Shirzaei performed the *in vitro* tests. Drs Sullivan, Gao, Stoppel, and Black helped with the *in vivo* and *ex vivo* studies and the manuscript revision. Drs Annabi, Khademhosseini, Noshadi, Hong, and Portillo-Lara wrote and revised the manuscript. Dr Tamayol revised the manuscript. Dr Shin assisted with the experimental design.

Acknowledgements

N. A. acknowledges support from the American Heart Association (AHA, 16SDG31280010), FY17 TIER 1 Interdisciplinary Research Seed Grants from the Northeastern University, and the startup fund provided by the Department of Chemical Engineering, College of Engineering at the Northeastern University. A. K. acknowledges funding from the National Institutes of Health (AR057837, DE021468, D005865, AR068258, AR066193, EB022403, and EB021148) and the Office of Naval Research Presidential Early Career Award for Scientists and Engineers (PECASE).

References

1 J. Radhakrishnan, U. M. Krishnan and S. Sethuraman, *Biotechnol. Adv.*, 2014, **32**, 449–461.

2 N. Annabi, J. W. Nichol, X. Zhong, C. Ji, S. Koshy, A. Khademhosseini and F. Dehghani, *Tissue Eng., Part B*, 2010, **16**, 371–383.
3 N. Annabi, A. Tamayol, J. A. Uquillas, M. Akbari, L. E. Bertassoni, C. Cha, G. Camci-Unal, M. R. Dokmeci, N. A. Peppas and A. Khademhosseini, *Adv. Mater.*, 2014, **26**, 85–123.
4 M. W. Curtis and B. Russell, *J. Cardiovasc. Nurs.*, 2009, **24**, 87–92.
5 H. Tan and K. G. Marra, *Materials*, 2010, **3**(3), 1746–1767.
6 Y. Li, J. Rodrigues and H. Tomas, *Chem. Soc. Rev.*, 2012, **41**, 2193–2221.
7 G. Camci-Unal, N. Annabi, M. R. Dokmeci, R. Liao and A. Khademhosseini, *NPG Asia Mater.*, 2014, **6**, e99.
8 Q. V. Nguyen, D. P. Huynh, J. H. Park and D. S. Lee, *Eur. Polym. J.*, 2015, **72**, 602–619.
9 N. Annabi, S. M. Mithieux, P. Zorlutuna, G. Camci-Unal, A. S. Weiss and A. Khademhosseini, *Biomaterials*, 2013, **34**, 5496–5505.
10 N. Annabi, S. Selimovic, J. P. Acevedo Cox, J. Ribas, M. Afshar Bakooshli, D. Heintze, A. S. Weiss, D. Cropek and A. Khademhosseini, *Lab Chip*, 2013, **13**, 3569–3577.
11 N. Annabi, K. Tsang, S. M. Mithieux, M. Nikkhah, A. Ameri, A. Khademhosseini and A. S. Weiss, *Adv. Funct. Mater.*, 2013, **23**, 4950–4959.
12 Y. N. Zhang, R. K. Avery, Q. Vallmajo-Martin, A. Assmann, A. Vegh, A. Memic, B. D. Olsen, N. Annabi and A. Khademhosseini, *Adv. Funct. Mater.*, 2015, **25**, 4814–4826.
13 N. Annabi, S. R. Shin, A. Tamayol, M. Miscuglio, M. A. Bakooshli, A. Assmann, P. Mostafalu, J. Y. Sun, S. Mithieux, L. Cheung, X. S. Tang, A. S. Weiss and A. Khademhosseini, *Adv. Mater.*, 2016, **28**, 40–49.
14 Y. C. Chen, R. Z. Lin, H. Qi, Y. Yang, H. Bae, J. M. Melero-Martin and A. Khademhosseini, *Adv. Funct. Mater.*, 2012, **22**, 2027–2039.
15 J. W. Nichol, S. T. Koshy, H. Bae, C. M. Hwang, S. Yamanlar and A. Khademhosseini, *Biomaterials*, 2010, **31**, 5536–5544.
16 K. Yue, G. Trujillo-de Santiago, M. M. Alvarez, A. Tamayol, N. Annabi and A. Khademhosseini, *Biomaterials*, 2015, **73**, 254–271.
17 R. Z. Lin, Y. C. Chen, R. Moreno-Luna, A. Khademhosseini and J. M. Melero-Martin, *Biomaterials*, 2013, **34**, 6785–6796.
18 S. J. Bryant, C. R. Nuttelman and K. S. Anseth, *J. Biomater. Sci., Polym. Ed.*, 2000, **11**, 439–457.
19 X. Kong, S. K. Mohanty, J. Stephens, J. T. Heale, V. Gomez-Godinez, L. Z. Shi, J. S. Kim, K. Yokomori and M. W. Berns, *Nucleic Acids Res.*, 2009, **37**, e68.
20 C. Kielbassa, L. Roza and B. Epe, *Carcinogenesis*, 1997, **18**, 811–816.
21 R. Prasad and S. K. Katiyar, *Photochem. Photobiol.*, 2016, **93**, 930–936.
22 R. Sato, R. Harada and Y. Shigeta, *Biophys. Physicobiol.*, 2016, **13**, 311–319.
23 N. E. Fedorovich, M. H. Oudshoorn, D. van Geemen, W. E. Hennink, J. Alblas and W. J. Dhert, *Biomaterials*, 2009, **30**, 344–353.
24 L. Fodor, Y. Ullmann and M. Elman, *Aesthetic applications of intense pulsed light*, Springer, London, 2011.
25 H. Shih, A. K. Fraser and C. C. Lin, *ACS Appl. Mater. Interfaces*, 2013, **5**, 1673–1680.
26 Y. Hao, H. Shih, Z. Munoz, A. Kemp and C. C. Lin, *Acta Biomater.*, 2014, **10**, 104–114.
27 A. Fu, K. Gwon, M. Kim, G. Tae and J. A. Kornfield, *Biomacromolecules*, 2015, **16**, 497–506.
28 J. Hu, Y. Hou, H. Park, B. Choi, S. Hou, A. Chung and M. Lee, *Acta Biomater.*, 2012, **8**, 1730–1738.
29 S. B. Seif-Naraghi, J. M. Singelyn, M. A. Salvatore, K. G. Osborn, J. J. Wang, U. Sampat, O. L. Kwan, G. M. Strachan, J. Wong, P. J. Schup-Magoffin, R. L. Braden, K. Bartels, J. A. DeQuach, M. Preul, A. M. Kinsey, A. N. DeMaria, N. Dib and K. L. Christman, *Sci. Transl. Med.*, 2013, **5**, 173ra125.
30 A. Hasan, A. Khattab, M. A. Islam, K. A. Hweij, J. Zeitouny, R. Waters, M. Sayegh, M. M. Hossain and A. Paul, *Adv. Sci.*, 2015, **2**, 1500122.
31 X. Y. Li, T. Wang, X. J. Jiang, T. Lin, D. Q. Wu, X. Z. Zhang, E. Okello, H. X. Xu and M. J. Yuan, *Cardiology*, 2010, **115**, 194–199.
32 M. Plotkin, S. R. Vaibavi, A. J. Rufaihah, V. Nithya, J. Wang, Y. Shachaf, T. Kofidis and D. Seliktar, *Biomaterials*, 2014, **35**, 1429–1438.
33 P. Occhetta, R. Visone, L. Russo, L. Cipolla, M. Moretti and M. Rasponi, *J. Biomed. Mater. Res., Part A*, 2015, **103**, 2109–2117.
34 D. W. Lim, D. L. Nettles, L. A. Setton and A. Chilkoti, *Biomacromolecules*, 2008, **9**, 222–230.
35 C.-C. Lin, C. S. Ki and H. Shih, *J. Appl. Polym. Sci.*, 2015, **132**, 41563.
36 A. Metters and J. Hubbell, *Biomacromolecules*, 2005, **6**, 290–301.
37 C. S. Bahney, T. J. Lujan, C. W. Hsu, M. Bottlang, J. L. West and B. Johnstone, *Eur. Cells Mater.*, 2011, **22**, 43–55; discussion 55.
38 N. Annabi, A. Fathi, S. M. Mithieux, P. Martens, A. S. Weiss and F. Dehghani, *Biomaterials*, 2011, **32**, 1517–1525.
39 N. Annabi, S. M. Mithieux, A. S. Weiss and F. Dehghani, *Biomaterials*, 2010, **31**, 1655–1665.
40 P. Zorlutuna, N. Annabi, G. Camci-Unal, M. Nikkhah, J. M. Cha, J. W. Nichol, A. Manbachi, H. Bae, S. Chen and A. Khademhosseini, *Adv. Mater.*, 2012, **24**, 1782–1804.
41 A. P. Ebrahimi, *J. Vasc. Interv. Neurol.*, 2009, **2**, 155–162.
42 E. S. Fioretta, J. O. Fledderus, F. P. Baaijens and C. V. Bouten, *J. Biomech.*, 2012, **45**, 736–744.
43 A. Paul, A. Hasan, H. A. Kindi, A. K. Gaharwar, V. T. Rao, M. Nikkhah, S. R. Shin, D. Krafft, M. R. Dokmeci, D. Shum-Tim and A. Khademhosseini, *ACS Nano*, 2014, **8**, 8050–8062.
44 R. E. Akins Jr., D. Rockwood, K. G. Robinson, D. Sandusky, J. Rabolt and C. Pizarro, *Tissue Eng., Part A*, 2010, **16**, 629–641.
45 J. C. Ralphe and W. J. de Lange, *Trends Cardiovasc. Med.*, 2013, **23**, 27–32.

46 S. A. Shintani, K. Oyama, F. Kobirumaki-Shimozawa, T. Ohki, S. Ishiwata and N. Fukuda, *J. Gen. Physiol.*, 2014, **143**, 513–524.
47 D. J. Goldstein, *Histochem. J.*, 1969, **1**, 187–198.
48 Y. S. Heo and H. J. Song, *Ann. Dermatol.*, 2011, **23**, 44–52.
49 S. X. Liang and W. D. Phillips, *Anat. Rec.*, 2013, **296**, 184–191.
50 J. Liu, Y. Wang, W. Du and B. Yu, *Inflammation*, 2013, **36**, 738–749.
51 R. Z. Lin, Y. C. Chen, R. Moreno-Luna, A. Khademhosseini and J. M. Melero-Martin, *Biomaterials*, 2013, **34**, 6785–6796.
52 K. E. Sullivan, K. P. Quinn, K. M. Tang, I. Georgakoudi and L. D. Black 3rd, *Stem Cell Res. Ther.*, 2014, **5**, 14.